Performance characterisation of MPD thrusters

T. R. Nada
National Authority for Remote Sensing and Space Sciences
Cairo, Egypt

ABSTRACT

This paper introduces a characterisation of the performance indices and operating limits of the self field magnetoplasmadynamic thruster. The thrust, specific impulse, and efficiency are considered as the main performance indices, while the operating limits are the cathode lifetime, onset phenomenon, and the overfed state of the thruster. The effects of thruster parameters (current, mass flow rate, geometry, and propellant type) on the performance indices and operating limits are examined using one-dimensional model of cylindrical self-field thrusters. Design charts are presented to help the designers to choose the optimum and safe set of the thruster parameters that realise certain mission requirements.

NOMENCLATURE

A	area (m^2)
B	magnetic field strength (T)
C_T	thrust coefficient
f	force density (N/m^2)
I_{SP}	specific impulse (s)
I_{tot}	total impulse (N.s)
j	current density (A/m^2)
J	total current (A)
L	length (cm)
M	molecular weight (kg/kmol)
$\dot{m}$	mass flow rate of propellant (kg/s)
r	radius (cm)
R_m	magnetic Reynolds number
T	total thrust (N)]
u	velocity (m/s)
V	discharge volt (V)
x	co-ordinate
ξ	non dimensional current
γ	specific heat ratio
η_f	thruster efficiency
ε_i	first ionization potential (eV)
μ_o	permeability of free space = $4\pi\times10^{-7}$ (Henries/m)

Subscripts

a	anode
ar	argon
c	cathode
pr	propellant
Z, r, θ	radial system co-ordinates

Abbreviations

MPD	magnetoplasmadynamic
MHD	magneto hydro dynamic

Paper No. 3136. Manuscript received 27 September 2006, revised 19 March 2007, accepted 8 May 2007.

https://doi.org/10.1017/S000192400000470X Published online by Cambridge University Press

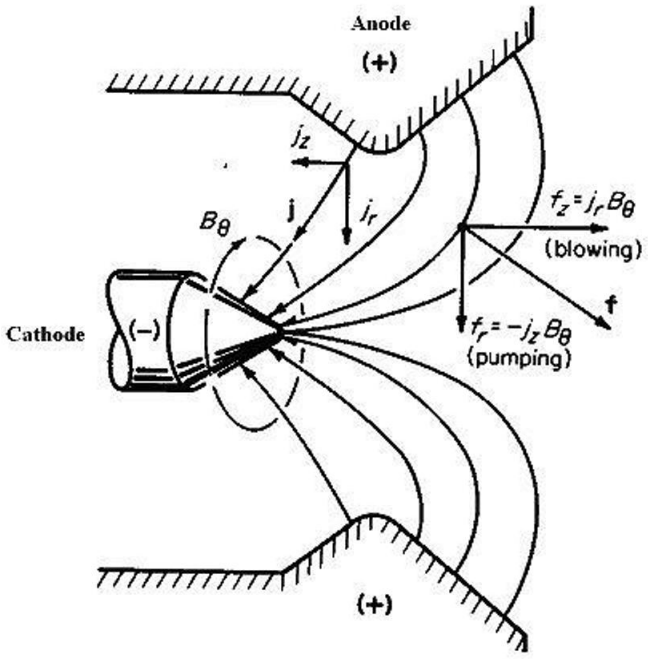


Figure 1. Schematic of self-field magnetoplasmadynamic thruster[2].

1.0 INTRODUCTION

The magnetoplasmadynamic (MPD) thruster is an electric propulsion device which has been proposed for a variety of mission applications, ranging from orbit raising maneuvers to robotic and piloted multi-megawatt planetary expeditions. Steady-state MPD thrusters have been operated at power levels approaching 600kW[1], while pulsed, quasi-steady devices have been operated in multi-megawatt power range[2]. The thruster is designed to provide low thrust with specific impulse (ISP) values of 1,000-10,000s, with the higher values corresponding to use of low molecular weight propellants.

Although simple in design and robust in operation, MPD thruster performance has typically been limited by low thrust efficiency in regimes of interest[3]. Severe electrode erosion has been observed at high values of specific impulse. This erosion is related to onset of significant discharge voltage oscillations and unsteady thruster operation[4-6]. Another limiting criterion is the thermo-ionic emission from the cathode[7-8]. The erosion rate from the cathode determines its lifetime and hence the mission duration of the whole thruster. On the opposite direction, lower levels of current lead to unstable operation of the thruster and this state are known as the overfed state. Modelling efforts of MPD thruster vary from simple one-dimensional[9-10] to the magneto-hydro-dynamic (MHD), two dimensional codes[11-12]. The one-dimensional models are simple and useful for characterising and optimising thruster performance as well as for system design and mission analysis.

Complete characterisation of the performance indices of MPD thruster has not been investigated yet for various space missions. These indices include thruster efficiency, specific impulse, and produced thrust level as functions of mass flow rate, current level, propellant type, and thruster geometry. Also, the effect of operating limits such as the onset phenomenon, cathode lifetime, and overfed of the thruster on the optimisation of thruster for certain mission are not published elsewhere.

In this paper, firstly, the existing one-dimensional models are reviewed and their results are compared to experimental work at various operating regimes. The ranges of validation for these models are identified. The onset phenomenon, cathode lifetime, and thruster overfed limits are then introduced as the main operating limits. Design charts for performance indices (efficiency, specific impulse, and thrust level) while employing different propellants, mass flow rates, geometry, and levels of current are presented. The trends of performance indices are discussed and explained. This is useful for system design and mission analysis and is essential for preliminary design of spacecraft employing MPD thrusters.

2.0 MPD THRUSTER TECHNOLOGY

The MPD thruster, shown schematically in Fig. 1, is essentially coaxial device in which a high-current discharge ionizes and accelerates gas to high exhaust velocities through the action of the Lorentz-force produced by the interaction between the current flowing through the plasma and self-induced or applied magnetic field. The schematic in the figure shows the self-field version with no applied magnetic field. Two main forces exist. First, axial acceleration (blowing) is provided by the crossing of the radial arc current with the self-generated azimuthally magnetic field. Second, is the electromagnetic pumping process; the axial components of arc current cross with azimuthally magnetic field to establish a radial gradient in the gas dynamic pressure.

At high currents, the pumping component causes traveling of charge carriers towards thruster axis and depletion or decrease of these carriers near the anode. This produces an increase in plasma resistance and hence increases the discharge voltage for the same current level. Electrode ablation and severe oscillations in discharge voltage are noticed at these conditions. This is called the onset phenomenon which is a main limit for the performance of MPD thrusters.

3.0 MPD THRUSTER MODELS

It is useful to have simple analytical model that can readily be employed to predict the thrust, specific impulse, and efficiency of MPD thrusters for wide range of operating parameters such as current, mass flow rate, geometry, and propellant type. During last three decades some models were introduced. Hereafter, these models are reviewed and compared with experimental work to reveal their validation regimes.

3.1 Maecker formula

The most simple and earliest formulation is the Maecker formula[13], which states that

$$T = \frac{\mu_o}{4\pi}\left[\ln\left(r_a/r_c\right) + \frac{3}{4}\right]J^2 \qquad \ldots (1)$$

On this equation, the thrust (T) is a function of anode radius (r_a), cathode radius (r_c), and electric current (J). The constant (μ_o) is the permeability of free space and has the value of ($4\pi\times10^{-7}$ Henries/m). A dimensionless thrust coefficient, C_T, represents some kind of scaling for the thruster performance. This coefficient is usually employed to characterise the thruster performance and has the order of unity. It can be defined as:

$$C_T = \frac{4\pi}{\mu_o}\left(\frac{T}{J^2}\right) \qquad \ldots (2)$$

For the case of Maecker formula, this coefficient is

$$C_T = \ln\left(\frac{r_a}{r_c}\right) + \frac{3}{4} \qquad \ldots (3)$$

https://doi.org/10.1017/S000192400000470X Published online by Cambridge University Press

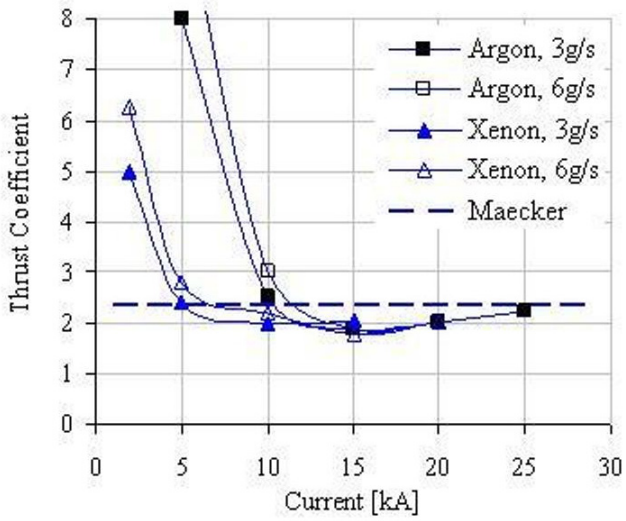


Figure 2. Comparison of the Maecker thrust coefficient with measurements[14-16].

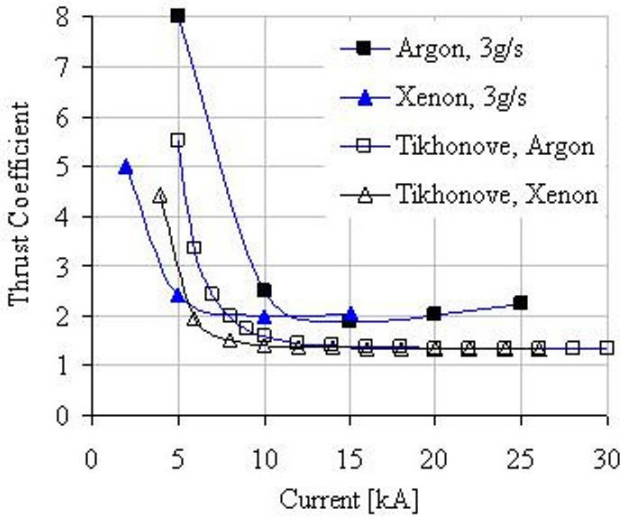


Figure 3. Tikhonov and measured C_T for argon and xenon.

It is obvious from this formula that the thrust coefficient is independent of current, mass flow rate, and propellant type. Therefore, this model always contradicts with experimental measurements. Figure 2 shows the thrust coefficient calculated according to the Maecker formula and that estimated from thrust measurements taken from Refs 14-16 for Argon and Xenon at mass flow rates of 3 and 6 g/s. The thruster geometry is set similar to that of Princeton full scale bench mark thruster[9]. It is clear from this figure that the Maecker model does not account for the thrust modeling of real MPD thrusters with different propellants and mass flow rates and give no change of thrust coefficient with current. However, the Maecher model gives reasonable predictions at high current, which is the regime of interest for high specific impulse.

A similar model was derived by Toki[10]. This model employed a simple quasi-one-dimensional representation for the self-field MPD thruster to demonstrate the existence of an optimum geometry that produces maximum thrust for fixed current, voltage, mass flow rate, and thruster length. The model, which is similar to that of Kuriki *et al*[17], is highly idealised; in particular, the energy equation is not included in the relevant equations. The problem is ruled by two differential equations for the plasma velocity (u) and the magnetic flux (B):

$$\frac{\mathrm{d}u}{\mathrm{d}x} = R_m\left(V - AuB\right)B \qquad \ldots (4)$$

$$\frac{\mathrm{d}B}{\mathrm{d}x} = -R_m\left(\frac{V}{A} - uB\right) \qquad \ldots (5)$$

On this model, (R_m) is the magnetic Reynolds number, (V) is the discharge volume, and (A) is the channel area. The equations are expressed in nondimensional form[10], and the channel height is the problem control variable, while the objective function to be maximised is the exit velocity. Nevertheless this model was developed for channel with square cross section; it gives insight in the results of such analysis for cylindrical thrusters. Both (R_m) and (V), the two parameters in the model, can be assigned in advance when the channel geometry is sought (R_m = 10 and V = 4·7 are employed by Toki[10]), while they must be left free if the channel profile is assigned. The results of this model show constant thrust coefficient with variable current level for fixed geometry analogous to the results obtained from Maecker model. Moreover, it results in a very high value of thrust coefficient (~10) for geometry similar to that used to obtain the results presented in Fig. 2.

3.2 Tikhonov model

The Tikhonov[18] semi-empirical model characterises the case of cylindrical MHD channel flow in a simple expression for the thrust coefficient:

$$C_T = \frac{\gamma + 1}{2} + \frac{0{\cdot}5}{\alpha_o^2} \qquad \ldots (6)$$

The dimensionless parameter (α_o) is evaluated at the upstream end of the channel;

$$\alpha_o = \frac{\gamma \mu_o}{8\pi a_o}\frac{J^2}{\dot{m}} \qquad \ldots (7)$$

The ion acoustic speed (a_o) is calculated at electron temperature of 1·0eV[18] at upstream end. Figure 3 shows the Tikhonov thrust coefficient compared with the measured values for argon and xenon as propellants both at 3g/s flow rate. It is obvious from this figure that the Tikhononv thrust coefficient decreases with current and specifically with (J^{-4}) scaling. Also, this model reflects the effect of propellant type opposite to the rersults of Maecker and Toki approaches. However, at high currents, the thrust coefficient is almost constant and under predicts the actual values. This is apparent from Equations 6 and 7, as the current and (α_o) increase the thrust coefficient becomes constant with a value (γ+1)/2, which is nearly (1·33).

Figure 4 displays the variation of Tikhonov and measured thrust coefficients with current for argon as propellant at 3 and 6g/s flow rates. It is clear from this figure that the Tikhonov model produces an increasing in thrust coefficient as the mass flow rate increases at same current level especially at low level currents, and this trend is verified by the experimental results. On the other hand, the Tikhonov model under predicts the thrust coefficient for whole investigated current level at these mass flow rates. Thus, Tikhonov formula is considered as an improvement on Maecker formula. The thrust coefficient is not constant except at high currents and it reflects roughly the effects of propellant type and mass flow rate especially at low levels of current.

3.3 LaPointe model

LaPointe[19] developed a two-temperature code to simulate self-field MPD thrusters and tested this model against the experimental results of the Princeton University full-scale benchmark thruster operated

https://doi.org/10.1017/S000192400000470X Published online by Cambridge University Press

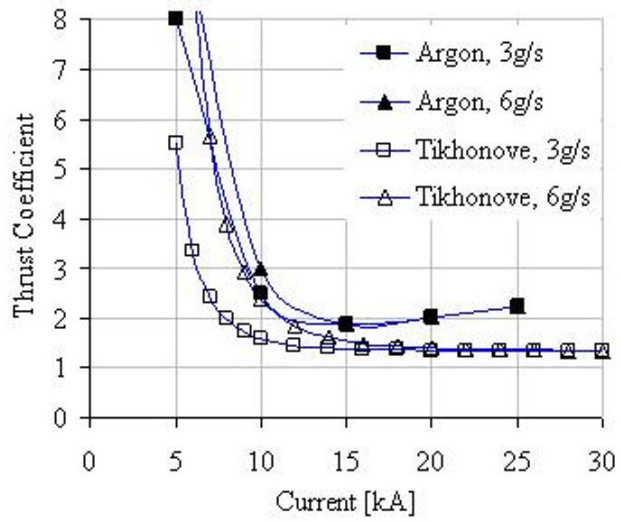


Figure 4. Tikhonov and measured C_T for argon at 3 and 6g/s.

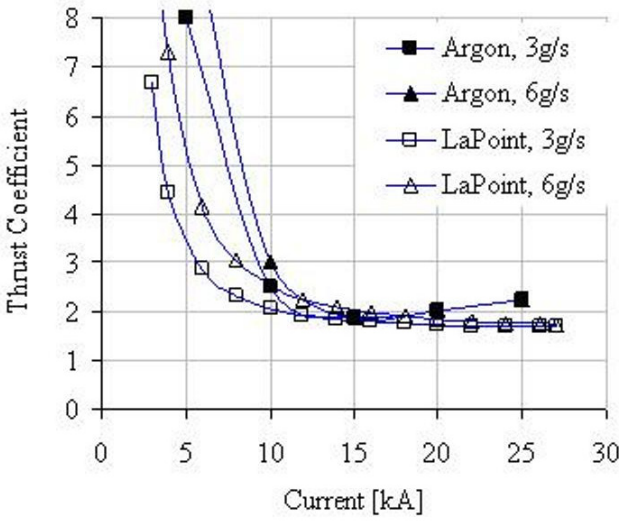


Figure 5. LaPoint and measured C_T for argon at 3 and 6g/s flow.

with argon and hydrogen as propellant and with that of the Osaka University MY-1 thruster operated with hydrogen. This comparison with experimental work verified the code for certain range of parameters and hence an analytical expression is derived by curve fitting routine to express total thrust as function of current (J), mass flow rate ($\dot{m}$), propellant molecular weight (M_{pr}), and thruster dimensions (r_a and r_c):

$$T = \frac{\mu_o}{4\pi} J^2 \left[\ell n \frac{r_a}{r_c} + \alpha \right] \left[\left(1{\cdot}52 - 0{\cdot}013 M_{pr} \right) + \left(33{\cdot}12 - 3{\cdot}19 M_{pr} + 0{\cdot}065 M_{pr}^2 \right) \frac{10^9 \dot{m}}{J^2} \right] \quad \ldots (8)$$

The parameter (α) depends on the assumed current distribution model (attachment at anode) and $0 \le \alpha \le 0{\cdot}75$, thus the thrust coefficient is:

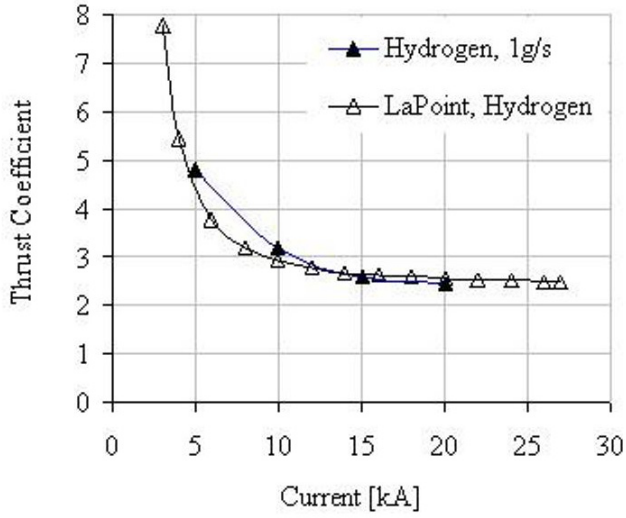


Figure 6. LaPoint and measured C_T for hydrogen.

$$C_T = \left[\ell n \frac{r_a}{r_c} + \alpha \right] \left[\left(1{\cdot}52 - 0{\cdot}013 M_{pr} \right) + \left(33{\cdot}12 - 3{\cdot}19 M_{pr} + 0{\cdot}065 M_{pr}^2 \right) \frac{10^9 \dot{m}}{J^2} \right] \quad \ldots (9)$$

This equation is only applicable to self-field MPD thrusters with cylindrical (not flared) electrode designs and its validity is limited to geometries with:

$$r_c \ge 0{\cdot}5\text{cm}, \; r_a \ge 2{\cdot}5\text{cm}, \; 5{\cdot}0 \le \frac{r_a}{r_c} \le 10, \; \frac{L_a}{r_a} \le 5, \text{ and } L_a \approx L_c \quad \ldots (10)$$

Figures 5 and 6 present the results of this model (using $\alpha = 0$) compared to the experimental results. It is clear from Fig. 5 that this model adopts well with the variation of thrust coefficient with current and mass flow rate for argon as propellant especially at high current levels. At low current levels the model significantly under predicts the measured thrust coefficient, indicating that the simple thrust equation does not accurately account for thermal acceleration.

However, the model becomes progressively more accurate at high current levels, indicating that it may still be applicable at current levels of interest. Figure 6 shows comparison of the model results with experimental for hydrogen as propellant. It clears that the model still predicts well the thrust at high current levels even with different propellants. This model was derived only for argon and hydrogen as propellants, thus when it is employed for other propellants as xenon it fails to predict the thrust as it is obvious from Fig. 7.

3.4 Choueiri model

The Choueiri[9] model introduces the thrust coefficient of self-field MPD thruster in semi empirical formulation in which the contributions of blowing and pumping thrust are considered. The model states that

$$C_T = \frac{\dot{m}}{\dot{m}^* \xi^4} + \ln \left[\frac{r_a}{r_c} + \xi^2 \right] \quad \ldots (11)$$

https://doi.org/10.1017/S000192400000470X Published online by Cambridge University Press

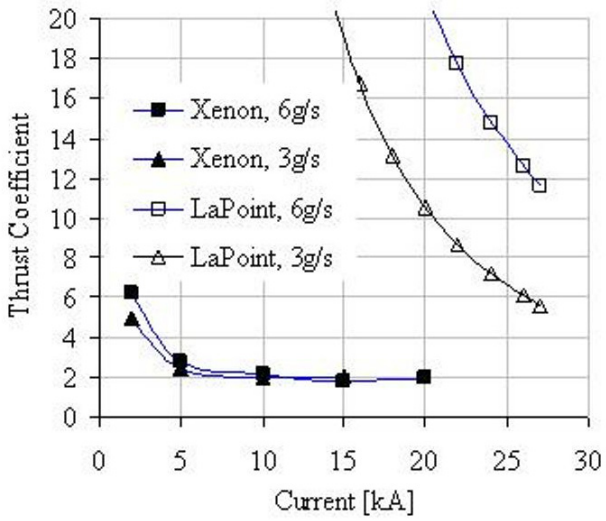


Figure 7. LaPoint and measured C_T for xenon at different mass flow rate.

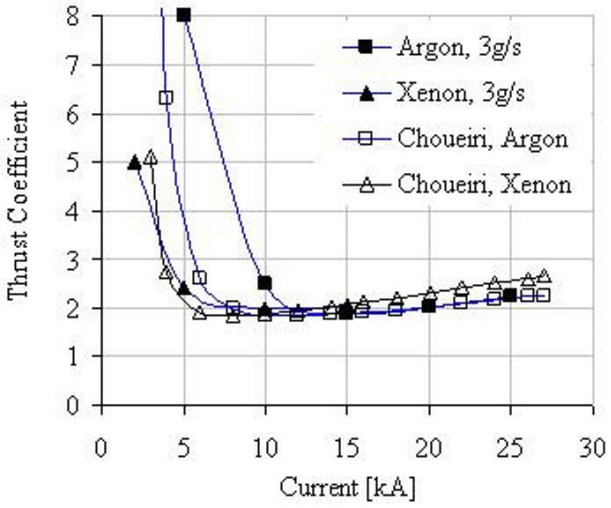


Figure 8. Choueiri and measured C_T for argon and xenon at 3g/s flow.

The dimensionless current (ξ) is expressed by:

$$\xi = \frac{J\left(\frac{\mu_o}{4\pi}\ln\frac{r_a}{r_c}\right)^{0.5}}{\dot{m}^{0.5}\left(2\varepsilon_i / M\right)^{0.25}} \quad \ldots (12)$$

The (M & ε_i) are mass and first ionization potential of the neutral atom of the propellant, respectively. Applying the model to the data of argon with mass flow rate of (6g/s), yielded ($\dot{m}^* = 66$g/s)[9]. Then, applying this value for the data of both argon and xenon at three different mass flow rates as well as for two similar thrusters with different length scales, Choueiri proves that the ($\dot{m}^*$) is a universal mass flow rate and equals 66g/s. This means that this value does not change with mass flow rate, propellant type, or thruster geometry.

Figure 8 shows the variation of thrust coefficient of Choueiri model compared to experimental results for both argon and xenon as propellant at 3g/s mass flow rate. The agreement of the model with experimental results is good especially at high currents, while at low currents, the agreement for xenon is better than that for argon. Figure 9 presents the same comparison but for argon at both 3 and 6g/s mass flow rates. The agreement of the model with experiments is fairer at high mass flow rates than at low mass flow rates.

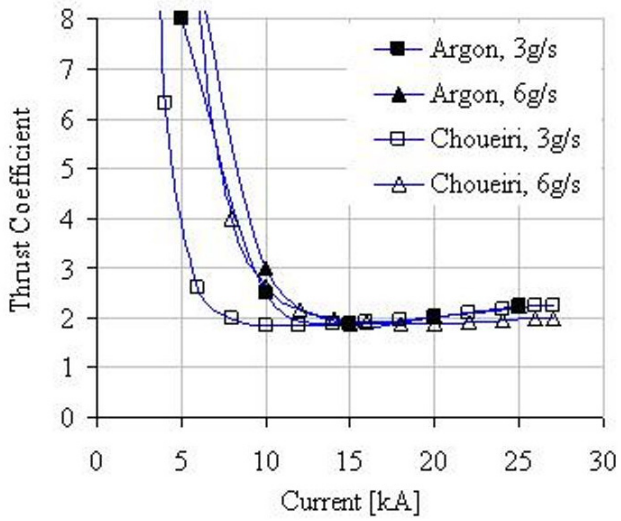


Figure 9. Choueiri and measured C_T for Argon at 3 and 6g/s flow.

From the above review of the existing one-dimensional models for the MPD thruster, it is apparent that the Choueiri model is the most accurate one of those assessed. It gives variations of thrust coefficient with current, propellant mass flow rate, thruster geometry, and propellant type. These are the main four parameters for optimisation of the MPD thruster. This model will be employed in the following sections to investigate the effects of thruster parameters on performance indices of MPD thrusters.

4.0 THRUSTER OPERATING LIMITS

Mainly, there are three limiting phenomena for the MPD thruster, named thermo-ionic emission from the cathode, onset phenomenon at high specific impulse, and overfed conditions. The cathode is the most likely component to fail if operation is not conducted above the onset condition. Discharge current is sustained by thermo-ionic emission from the cathode, and if not properly sized the evaporation of cathode material leads to limited thruster life. Also, quasi-steady state operation results in higher erosion rates than that for steady state operation because of the cold starts of cathode[6]. Therefore, the lifetime of pulsed MPD thrusters is generally lower than that of the steady state ones. This lifetime would be extended by the use of an externally heated cathode featuring low work function material[20].

Reported erosion rates for steady state thrusters vary from 0·03μg/C[8] to 0C_T18μg/C[7] and can be lowered to range of (~2·0ng/C) by using pure propellant or by employing deoxygenating device[7]. The erosion rates for quasi steady-state thruster operation were measured in the range from 3·4μg/C[6] to 10μg/C[7] or 13μg/C[21] and it is a function of propellant type[6] and geometry[22]). Experimental investigations for the effect of propellant molecular weight on cathode erosion rate showed that the erosion rate clearly decreases with the molecular weight increased[23]. This fact may be attributable to the cathode bombardment by the atom of higher mass which facilitates electron emission so that localised heating is thereby avoided.

The study will focus on quasi steady-state operation because the quasi-steady MPD thruster performance will be slightly worse than steady-state thruster under the same operating conditions. In support of this approach, previous experiments performed on MPD thrusters demonstrated that pulsed thrusters operated at up to several hundred kilowatts provided lower thrust and higher voltage than identical thrusters operated at comparable steady-state power levels[24]. This is because the pulsed thruster suffers from the power deposited in anode heating to release electrons from its surface at each pulse.

https://doi.org/10.1017/S000192400000470X Published online by Cambridge University Press

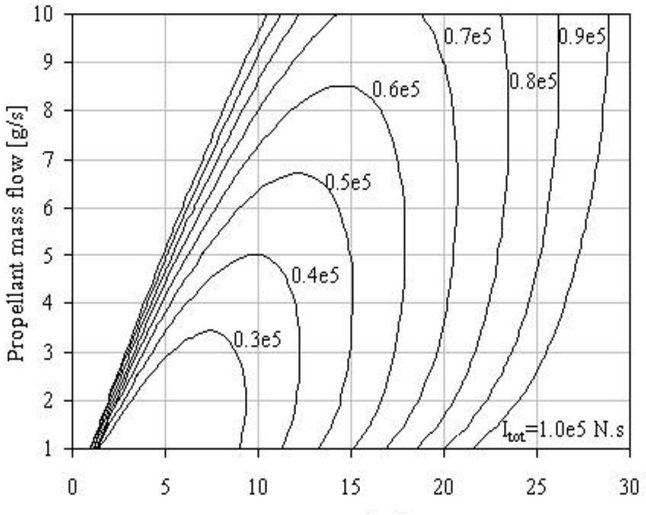


Figure 10. Velocity change contours on current-mass flow chart.

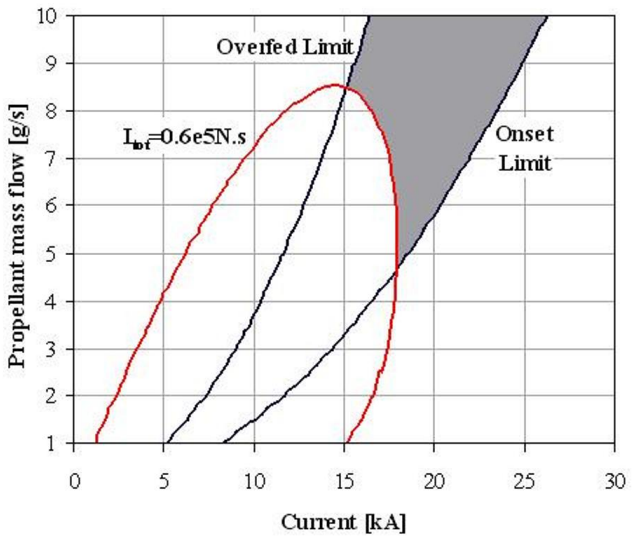


Figure 11. Operating limits of MPD thruster.

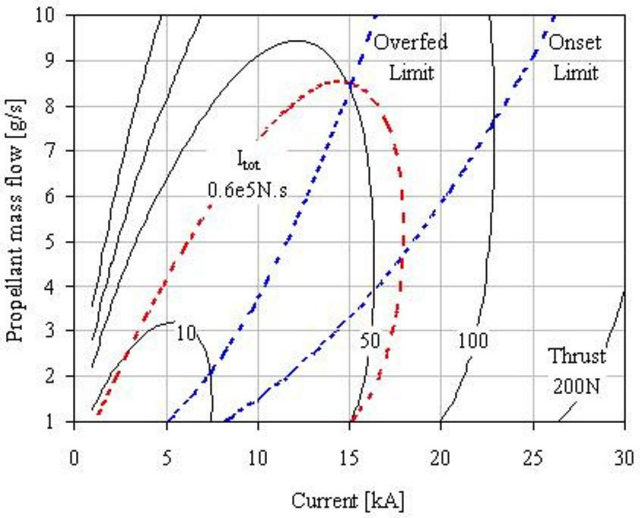


Figure 12. Thrust contours and operating limits for argon.

Alternatively, this power is only needed for the starting of a steady state thruster. The plasma resistance will be higher for pulsed thruster, due to cold starting, than that for steady state one and hence the discharge voltage will be higher at the same current. Thus, thruster, which is optimized under quasi-steady state operation, will be more efficient when work under steady state operation.

An erosion rate of (3·4μg/C), which is the most optimistic value taken from the literature, is employed. This rate could be justified by the use of a heated cathode incorporating material of low work function. From thruster geometry, the cathode volume is calculated, then, employing tungsten material for the cathode, the cathode mass is evaluated. Assuming that 10% cathode mass loss is the end of life criterion[6], the total electric charge is obtained via:

$$total\ charge = 0{\cdot}1\frac{cathode\ mass}{erosion\ rate} \qquad \ldots (13)$$

At each current (J), the lifetime is calculated as:

$$time = \frac{total\ \ charge}{current} \qquad \ldots (14)$$

For quasi-steady state operation and assuming that the cathode lifetime is the end of life criterion for the whole thruster, the total impulse is simply the thrust multiplied by this time. Figure 10 presents the contours of constant total impulse (I_{tot}) for thruster employing argon propellant and having cathode and anode lengths equal to 10cm, cathode radius equals to 0·95cm and anode to cathode radius ratio equals to 5.

This geometry is employed because a comprehensive measured performance data is available for this thruster and hence the efficiency contours can be added to the chart as will be discussed in the next section of this paper[15]. These contours are plotted on a chart of current-mass flow rate which are the main two parameters of the thruster design with a certain geometry and propellant type. It is clear from this figure that the values of current and propellant mass flow rate must be chosen external to the closed contour of certain total impulse to achieve this impulse within the lifetime of the thruster.

It was found that below certain level of ($J^2/\dot{m}$) the thruster is 'overfed' and undergoes erosive conditions. This occurs at low current and/or high mass flow rate. Low current results in decreased emitted electrons, while high mass flow rate produces high dense plasma within the discharge passage. At these conditions, the plasma plume is very unsteady and the cathode has orange/yellow color and obviously does not emit electrons efficiently. Myers *et al*[25] has suggested that the overfed regime occurs at ($J^2/\dot{m} \leq 2{\times}10^{10}$ ($A^2s\ kg^{-1}$), while Wood *et al*[26] measured it at ($J^2/\dot{m} \leq 2{\cdot}7{\times}10^{10}$ ($A^2s\ kg^{-1}$).This limit is indicated in Fig. 11 employing ($J^2/\dot{m} = 2{\cdot}7{\times}10^{10}$ ($A^2s\ kg^{-1}$).

The onset phenomenon limits the MPD thruster performance. This phenomenon collectively refers to increased erosion of thruster components and large voltage oscillations at a critical current with a fixed mass flow and geometry. Onset was first observed experimentally and since then, there have been several theoretical attempts to understand and quantify it[4]. The onset is related to increasing ($J^2/\dot{m}$) and it has been extensively documented. Reference (19) presents a formulation for the relation between the maximum stable ($J^2/\dot{m}$) and thruster geometry and propellant molecular weight as

$$\frac{J^2}{\dot{m}} \leq \frac{6{\cdot}25\times10^9}{r_c}\left(\frac{L_c}{L_a}\right)\left(\frac{M_{ar}}{M_{pr}}\right)^{0.57} \times \left[5-\left(\frac{L_a}{r_a}\right) + 4\left(\frac{10r_c - r_a}{2{\cdot}5}\right)\right] \qquad \ldots (15)$$

This equation is subject to the same geometric constraints given by Equation 10. It represents a simple analytical formulation for the experimental results obtained from Princeton University full-scale benchmark thruster (cathode and anode lengths equal to 10cm,

https://doi.org/10.1017/S000192400000470X Published online by Cambridge University Press

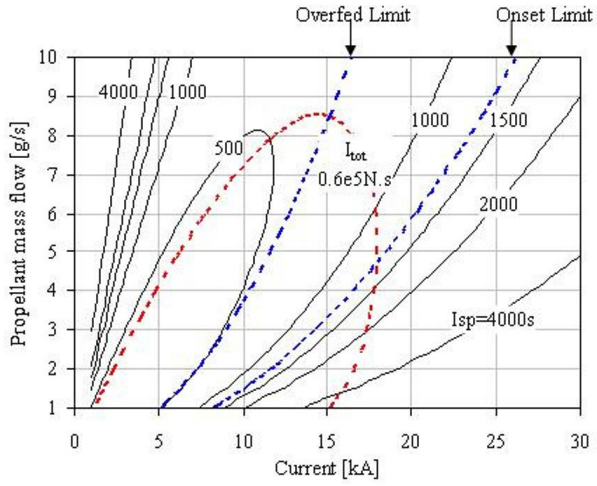


Figure 13. Specific impulse contours and operating limits for argon.

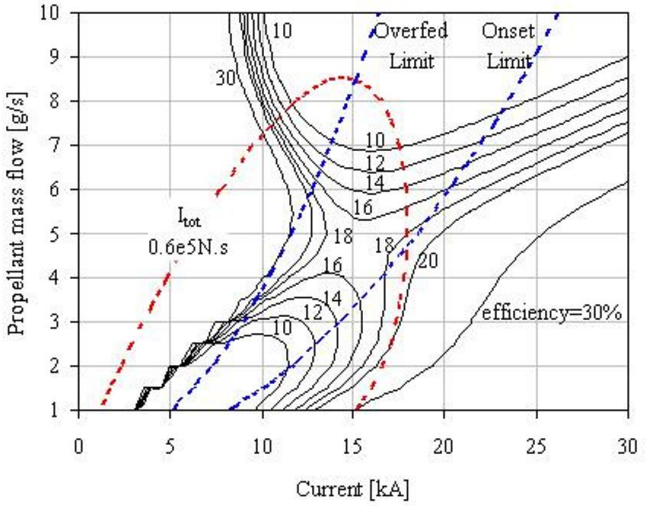


Figure 14. Efficiency contours and operating limits for argon.

cathode radius equals to 0·95cm, and anode to cathode radius ratio equal to 5) operating with argon and hydrogen and that obtained from Osaka University MY-1 thruster operated with hydrogen[19]. The line representing this limit and that representing the limit of overfed of the thruster are plotted in Fig. 11 for a thruster working with argon as propellant and having cathode and anode lengths equal to 10cm, cathode radius equals to 0·95cm, and anode to cathode radius ratio equal to 5. Also, the curve representing a total impulse of (I_{tot} = 0·6*e*5 N.s) is plotted in the same figure.

The chosen value of total impulse is suitable for the investigated range of current and mass flow rate and reflects an average of the values proposed by several missions[6]. These three curves represent the operating limits of the considered thruster. The shaded area, which is to the left of the onset limit, to the right of the overfed limit and outside the total impulse contour, represents the safe and adequate regime of work for this thruster if a mission with at least (I_{tot} = 0·6*e*5 N.s) is considered.

5.0 RESULTS AND DISCUSSIONS

The Choueiri model was employed to get the thrust coefficient and hence the thrust and specific impulse for the Princeton University full-scale benchmark thruster using argon as propellant, while the current and propellant mass flow rate were varied as parameters. This thruster has cathode and anode lengths equal to 10cm, cathode radius equals to 0·95cm and anode to cathode radius ratio equals to 5[15]. Figure 12 shows the contours of constant thrust on current-mass flow chart along with the operating limits. This figure indicates that this thruster can produce between (50N) and (130N) for the investigated range of mass flow rate and current.

The corresponding specific impulse contours are plotted on Fig. 13 together with the operating limits. It is seen from this figure that a maximum of (1,350s) of specific impulse can be obtained with this thruster design. The thruster efficiency is defined by the ratio between thrust power and electric power deposited into the plasma;

$$\eta_f = \frac{T^2}{2\dot{m} \cdot J \cdot V} \quad \ldots (16)$$

To date, there are no models to estimate the voltage at certain current. Therefore, the only way to evaluate the electric power deposited into the plasma and hence the thruster efficiency is the experimental measurements of voltage-current characteristics[11-12]. These characteristics are linear below the onset limit and vary with geometry, propellant mass flow rate and propellant type. Reference 15 presents voltage measurements with current for various mass flow rates of argon, xenon, and hydrogen for the Princeton University full-scale benchmark thruster. These results are used with linear interpolations between points to get the voltage and hence the thruster efficiency at certain current and propellant mass flow rate. The resulting efficiency contours alongside the operating limits are plotted on Fig. 14. It is seen from this figure that the maximum obtainable efficiency is nearly (19%) at a current of (18kA) and mass flow rate of (4·7g/s). This point matches a thrust of nearly (60N) and specific impulse of (~1,320s) as can be seen from Figs 12 and 13, respectively.

It is possible to get higher thrust level with nearly the same specific impulse but at the expense of efficiency. Sometimes on the mission analysis, it is required to do a maneuver on a minimum time and the available power is not the limiting factor. In such case, the designer can choose the upper limit of the thrust level which is nearly double the value at maximum efficiency (130N at efficiency of 5·2% compared with 60N at efficiency of 19%). Also, at this point the maximum obtainable total impulse during the thruster lifetime is higher (I_{tot} = 0·8×10^{5}N.s compared to I_{tot} = 0·6×10^{5}N.s). The opposite state is when the available power is the limiting factor and hence the maximum efficiency is required even on the expense of thrust level and hence on the mission time. It is worth to note that the specific impulse is nearly the same in the two cases.

The employment of another propellant with smaller molecular weight (such as hydrogen) and/or changing the thruster geometry can be used to move the onset limit to the right (higher maximum) and hence better performance is expected. However, the erosion rate increases with decreasing molecular weight[23] and thus a limited life is expected which means lower total impulse for the same thrust. Figure 15 presents the thrust contours and operating limits for the same thruster employing hydrogen as propellant for a range of (0·1-1·0g/s) propellant mass flow rate. This range of mass flow rate is determined by the availability of measurements given in Ref. 15. It is seen from this figure that to get a range of (60-100N) of thrust as that for argon, only (~0·2*e*5N.s) of total impulse can be reached within the lifetime. This is due to the high erosion rate, which is (11μg/C) for hydrogen[23] compared with (3.4μg/C) for argon. Also, it is clear from this figure that the overfed limit does not restrict the performance for the investigated range of current and mass flow rate.

The specific impulse contours are plotted in Fig. 16 together with the operating limits. This figure clearly shows that an order

https://doi.org/10.1017/S000192400000470X Published online by Cambridge University Press

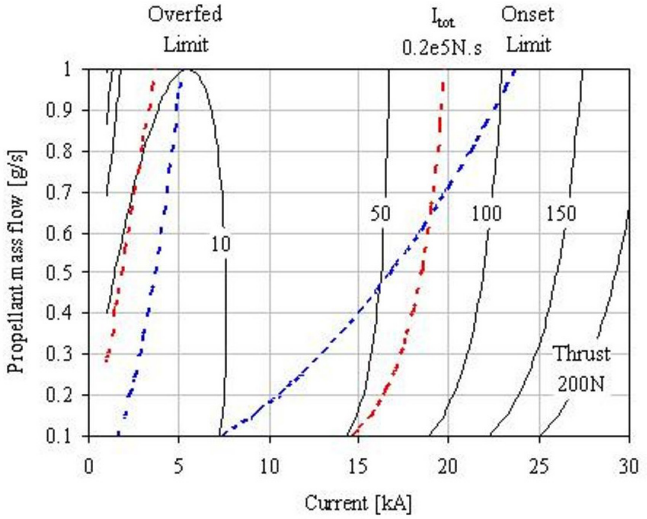


Figure 15. Thrust contours and operating limits for hydrogen.

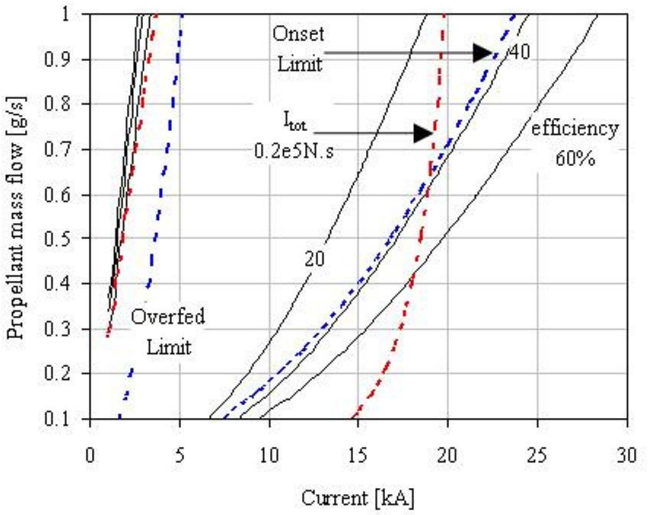


Figure 17. Efficiency contours and operating limits for hydrogen.

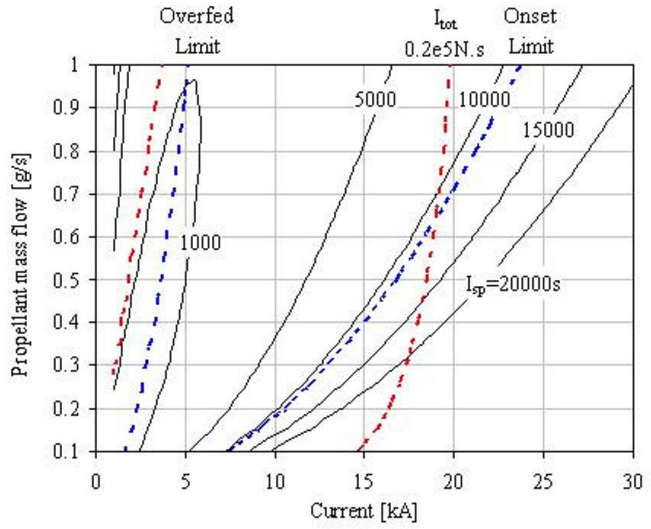


Figure 16. Specific impulse contours and operating limits for hydrogen.

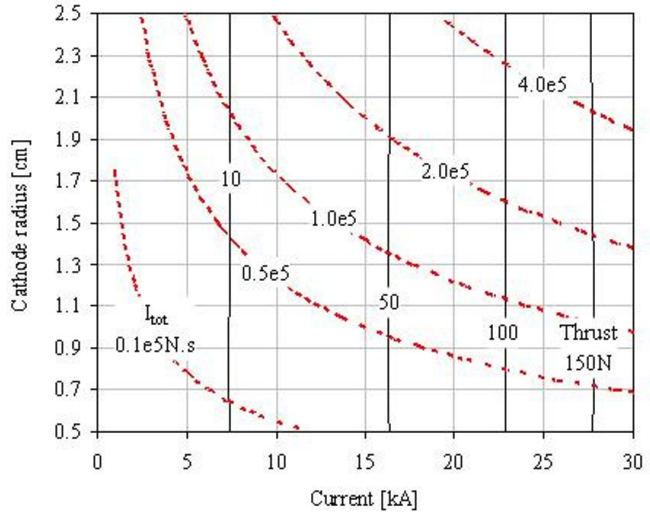


Figure 18. Cathode radius effects on thrust and total impulse, (r_a/r_c = 5·0).

of (11,000s) of specific impulse can be reached when employing hydrogen compared with only (1,350s) for argon. The efficiency contours and the performance limiting lines are plotted in Fig. 17. From this figure it is obvious that an efficiency of nearly (38%) can be obtained without any loss in specific impulse and also with the maximum obtainable thrust, which is (107N) for the investigated range of current and mass flow rate.

These promising results for the hydrogen as propellant must be considered in conjunction with the disadvantages of lower total impulse, which is only ($0{\cdot}2\times10^5$N.s) compared with ($0{\cdot}6\times10^5$N.s) or more for argon. Also, it was found that the use of hydrogen results in voltage fluctuations which may cause electromagnetic interference with communication devices in satellites[23]. Xenon has higher molecular weight than argon and thus it results in larger lifetime and hence higher total impulse, while the onset limit is more restricting the range of thrust and specific impulse. The obtained results for xenon are (~14%) efficiency, (~70N) thrust, and (~700s) specific impulse for mission of nearly ($2{\cdot}0\times10^5$N.s) total impulse.

It is seen from the above study that the onset phenomenon is always limiting the performance of the thruster and hence the thruster will have the maximum specific impulse, efficiency, and thrust near this limit. Moreover, it was noticed numerically[27] and verified experimentally[28] that optimum performance is obtained with nearly equal electrode lengths ($La \approx Lc$). Therefore, to investigate the geometry change effects, the cathode radius and anode to cathode ratio are changed with variation of current while the propellant mass flow rate is determined from the onset value of ($J^2/\dot{m}$).

Figure 18 presents the effect of varying cathode radius, with fixed anode to cathode ratio (r_a/r_c = 5·0), while using argon as propellant and other dimensions are similar to Princeton University full-scale benchmark thruster. It is obvious from this figure that the variation of cathode radius does not affect the thrust level, while the total impulse increases with increasing cathode radius for fixed current. These results of constant thrust are understandable from Fig. 9 and Equations 11 and 12 of the Choueiri model, which has no effect of varying cathode radius on thrust coefficient.

Moreover, the mass flow rate, which is determined from the value of maximum ($J^2/\dot{m}$), is nearly constant with variable cathode radius at small anode to cathode ratios. Also, the increase in total impulse is direct result of the increase in cathode radius. This is because increasing cathode radius leads to increase in

https://doi.org/10.1017/S000192400000470X Published online by Cambridge University Press

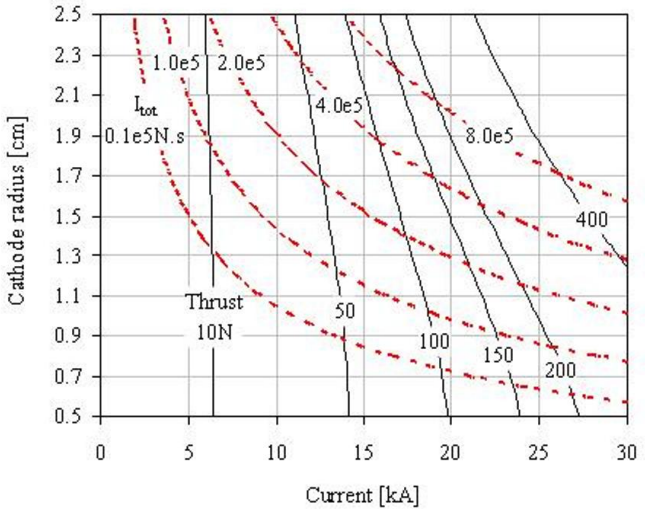


Figure 19. Cathode radius effects on thrust and total impulse, (r_a /r_c = 10·0).

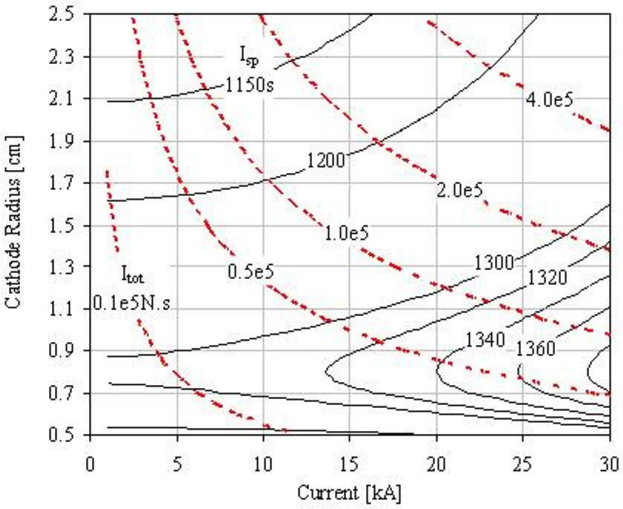


Figure 20. Cathode radius effects on specific impulse and total impulse, (r_a /r_c = 5·0).

cathode volume and mass, which leads to longer lifetime and hence higher total impulse at the same current level. Figure 19 presents the effect of varying cathode radius on thrust and total impulse if the ratio of anode radius to cathode radius is altered to (r_a/r_c = 10·0). This figure indicates that increasing cathode radius at constant current leads to increase in total impulse and slight increase in thrust. Also, higher levels of thrust and total impulse are obtainable with this high ratio of anode to cathode radii.

The effects of cathode radius on specific impulse with argon as propellant for (r_a/r_c = 5) and (r_a/r_c = 10·0) can be seen on Figs 20 and 21 respectively. It is seen from Fig. 20 that for this anode to cathode ratio and above specific impulse of (1,300s), there is a certain optimum cathode radius corresponds to the maximum specific impulse for certain current level, and this is at (r_c = 0·8cm). From Figs 20 and 21 it is apparent that for certain level of total impulse, it is recommended to work on high current and employ small cathode radius. However the effects of this trend on efficiency must be checked. Unfortunately, the thruster efficiency could not be evaluated for these changes on geometry as there are no experimental measurements for voltage-current characteristics with variation of cathode radius and ratio of anode to cathode radii.

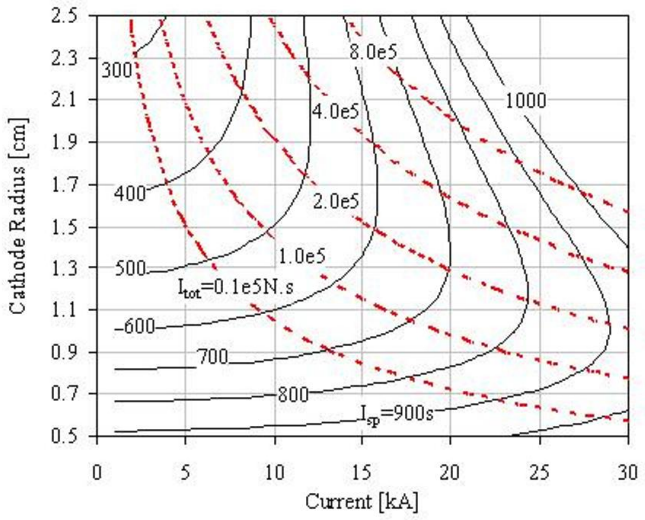


Figure 21. Cathode radius effects on specific impulse and total impulse, (r_a /r_c = 10·0).

6.0 CONCLUSIONS

The performance indices and operating limits of self-field magneto-plasmadynamic thruster are considered. The existing one-dimensional models are reviewed and their results are compared with experimental measurements. Of the investigated models, the Choueiri model seems to be the most accurate one. It is selected to investigate the effects of thruster parameters on thrust, specific impulse, and efficiency. The considered thruster parameters are current, propellant mass flow rate, propellant type, and geometry. Also, the effects of these parameters on onset phenomenon, cathode lifetime, and overfed condition are studied.

It was found that efficiency of (~20%) and specific impulse of (~1,300s) are obtainable for ranges of (1-30kA) of current and (1-10g/s) of propellant mass flow rate of argon. Alternatively, an efficiency of (~40%) and specific impulse of (~11,000s) are easily reached when employing hydrogen as propellant with mass flow rate of (0·1-1·0g/s) for the same range of current. The thrust is nearly the same for both argon and hydrogen, while the total impulse for argon is higher than that for hydrogen due to the lower cathode lifetime when employing hydrogen as propellant. Xenon gives poorer results in terms of efficiency, thrust, and specific impulse due to the restriction of onset phenomenon with xenon. While the obtainable total impulse is higher for xenon due to lower erosion rate of cathode material when employing xenon as propellant.

It is better to work on smaller cathode radius and larger current level to get high thrust and specific impulse for certain level of total impulse. Increasing the ratio of anode to cathode radii produces higher levels of both thrust and total impulse but in the expense of specific impulse for certain currents and cathode radii. The effect of geometry changes on thruster efficiency could not be investigated due to lack of experimental measurements of voltage-current characteristics.

REFERENCES

1. WINTER, M.W., NADA, T.R., AUWETER-KURTZ, M., HAAG, D. and FERTIG M. Investigation of nozzle geometry effects on the onset of plasma instabilities in high power steady state MPD thrusters, July 2006, 42nd AIAA/ASME/SAE/ASEE Joint Propulsion Conference & Exhibit, California, AIAA 2006-5016.
2. LAPOINT, M.R. High power MPD thruster performance measurements, September 2004, NASA TM-2004-213226.
3. FRUCHTMAN, A. Limits on the efficiency of several electric thruster configurations, *Physics of Plasma* May 2003, **10**, (5).

https://doi.org/10.1017/S000192400000470X Published online by Cambridge University Press

4. SUBRAMANIAM, V.V. and LAWLESS, J.L. Onset in magnetoplasmadynamic thrusters with finite-rate ionization, *J Propulsion and Power*, 1988, **4**, (6).
5 LAWLESS, J.L. and SUBRAMANIAM, V.V. Theory of onset in magnetoplasmadynamic thrusters, *J Propulsion and Power*, 1987, **3**, (2), pp 121-127.
6. SOVEY, J.S. and MANTENIEKS, M.A. Performance and lifetime assessment of magnetoplasmadynamic arc thruster technology, *J Propul and Power*, January-February 1991, **7**, (1), pp 71-83.
7. MYERS, R.M., SUZUKI, N., KELLY, A.J. and JAHN, R.G. Cathode phenomena in low power magnetoplasmadynamic thruster, *J Propul and Power*, 1991, **7**, (51), pp 760-766.
8. AUWETER-KURTZ, M. *et al*. Cathode phenomena in plasma thrusters, *J Propul and Power*, November-December 1993, **9**, (6), pp 882-888.
9. CHOUEIRI, E. Scaling of thrust in self-field magnetoplasmadynamic thrusters, *J Propul and Power*, 1998, **14**, (5), pp 744-753.
10. TOKI, K. Optimal control of quasi-one-dimensional self-field magneto plasma dynamic arcjet flowfields, *J Propul and Power*, 1997, **13**, (1).
11. SANKARAN, K., CHOUEIRI, E., and JARDIN, S.C. Comparison of simulated magnetoplasmadynamic thruster flowfields to experimental measurements, *J Propul and Power*, 2005, **21**, (1), pp 129-138.
12. HEIERMANN, J. and AUWETER-KURTZ, M. Numerical and experimental investigation of the current distribution in self-field magnetoplasmadynamic thrusters, *J Propul and Power*, 2005, **21**, (1), pp 119-128.
13. JAHN, R.G. *Physics of Electric Propulsion*, 1968, McGraw-Hill, New York.
14. BURTON, R.L., CLARK, K.E. and JAHN, R.G. Measured performance of a multi-megawatt MPD thruster, 1983, *J Spacecraft*, **20**, (3), pp 299-304.
15. CHOUEIRI, E.Y. and ZIEMER, J.K. Quasi-steady magnetoplasmadynamic thruster performance database, *J Propul and Power*, 2001, **17**, (5), pp 967-976.
16. LAPOINT, M.R., STRZEMPKOWSKI, E. and PENCIL E. High power MPD thruster performance measurements, NASA TM-2004-213226.
17. KURIKI, K., KUNII, Y. and SHIMIZU, Y. Idealized model for plasma acceleration in an MHD channel, *AIAA J*, 1983, **21**, (3), pp 322-326.
18. TIKHONOV, V.B., SEMENIHIN, S.A., ALEXANDROV, V.A., DYAKONOV, G.A. and POPOV, G.A. Research on plasma acceleration processes in self-field and applied field thrusters, 23rd International Electric Propulsion Conference, IEPC Paper 93-076.
19. LAPOINTE, M.R. Numerical simulation of cylindrical, self-field MPD thrusters with multiple propellants, 1994, NASA Contractor Report 194458.
20. DOMONKOS, M.T. *et al*, Preliminary pulsed MPD thruster performance, June 1995, 31st Joint Propulsion Conference, AIAA-95-2674.
21. KURTZ, H., AUWETER-KURTZ, M. and SCHRADE, H.O. Self-field MPD thruster design-experimental and theoretical investigations, September 1985, AIAA Paper 85-2002.
22. POLK, J.E., JASKOWSKY, W., KELLY, A.J. and JAHN, R.G. Measurement of MPD thruster erosion using surface layer activation, *J Propulsion and Power*, January-February 1987, **3**, (1), pp 33-38.
23. UEMATSU, K., MORIMOTO, S. and KURIKI, K. MPD thruster performance with various propellants, *J Spacecraft*, 1985, **22**, (4), pp 412-416.
24. LAPOINT, M.R. and MIKELLIDES, P.G. High power MPD thruster development at the NASA Glenn Research Center, August 2001, NASA CR-2001-211114.
25. MYERS R., KELLY A.J. and JAHN R.G. Electro thermal-electromagnetic hybrid thruster research, AIAA paper 87-1018.
26. WOOD, N.J., OSBORNE, J.J., ROBERTS, G.T. and GABRIEL, S.B. Characterization of a low-power steady-state magnetoplasmadynamic device for non-propulsive applications, *Plasma Sources Sci Technology*, 1997, **6**, pp 484-491.
27. LAPOINT, M. Numerical simulation of geometric scale effects in cylindrical self-field MPD thrusters, July 1999, NASA CR-1892242.
28. KING, D.Q. Magnetoplasmadynamic Channel Flow for Design of Coaxial MPD Thrusters, June 198, PhD dissertation, Princeton University2.

https://doi.org/10.1017/S000192400000470X Published online by Cambridge University Press